frontpage

assignment 1/2

assignment 2/2

ACKNOWLEDGEMENT

text....

SUMMARY

Text in English.

keywords:

text,text,text

SOUHRN

Text.

klíčová slova:

text,text,text

Contents

1 INTRODUCTION

Most of the newly discovered active pharmaceutical ingredients (APIs) are poorly water soluble in crystalline forms, which limit their bioavailability, dissolution, and then their distribution through the organism. This fact limits its wider oral use as a solid drug in medical treatment. Today, combinatorial chemistry techniques and high-throughput screening have led to a sharp increase in the quantity of nonsoluble API molecules, so the oral administration of poorly soluble drugs has become the biggest challenge for formulation scientists in the pharmaceutical industry. [1] There are different strategies to overcome this issue, such as cocrystal formation [2], conversion of API to its salt [3] or using solid dispersion. [4]

In 1961, Sekiguchi and Obi provided the earliest account of the so-called first-generation solid dispersion, when they discovered that the creation of eutectic mixtures enhances the rate of drug release and bioavailability. First-generation solid dispersions were built from crystalline carriers such as urea or sugars, forming crystalline solid dispersions. The second generation solid dispersion was replacing crystalline carriers by amorphous carriers such as polymers, forming an amorphous product in which crystalline API is dissolved. There exist also a third generation of solid dispersion using a surfactant carrier or a combination of amorphous polymers and surfactants. [5]

Our aim is to overcome the poor solubility by using amorphous solid phases of APIs and to avert the rearrangement of molecules into a crystal lattice. However, crystalline forms of APIs are advantageous because of their better stability during long-term storage and better predictions of changes at the molecular level under defined conditions, so the use of crystalline forms limits the bioavailibility. [6] The better solubility of APIs in amorphous forms comes from a higher Gibbs energy in the amorphous form compared to the crystalline forms. During processing, storage, and after contact with water or humidity, the thermodynamically metastable amorphous forms tend to crystallise. Solid mixtures of API and excipients (e.g. polymeric excipients) create amorphous solid dispersions (ASD) and offer a way to inhibit crystallisation of the API before and after oral administration of the dose. [7]

The addition of an excipient to an amorphous API can generally have a twofold effect on the rate of solid-state crystallisation, affecting both thermodynamic and kinetic aspects. Thermodynamically, it reduces the Gibbs energy due to strong intermolecular interactions between API and its excipient, as well as it increases kinetic barriers to recrystallisation. On the atomic scale of individual interactions, hydrogen bonding makes the most contribution. [8]

1.1 Studied compounds

1.1.1 Polylactic acid

Polylactic acid (PLA) was chosen as a biocompatible polymer excipient. PLA is a biodegradable polymer formed by the polymerisation of lactic acid. The formula of the PLA monomer unit is shown in Figure 1. In this work, two condensed units of D-PLA were considered as the simplest building block for creating all of the other longer polymer chains. Polymer samples of a length of 100 dimer units were created by replicating these dimer units. The molar weight of our dimer unit considered in the investigation (two polymerised lactic acid chains) is $M_w = 162.14 \, \text{g} \cdot \text{mol}^{-1}$, which means that the polymer chain used in the simulations has a molar weight equal to $M_w = 14 \, 431 \, \text{g} \cdot \text{mol}^{-1}$. Other suitable biocompatible and biodegradable polymers for ASD could be polyethylene glycol (PEG) and polyvinylpyrrolidone (PVP). [9]

Figure 1: PLA formula on the left, PLA dimer block representing the chain unit used to build up polymer chain in the middle and a PLA chain containing 100 dimer block used to create mixtures with APIs on the right.

1.1.2 Active pharmaceutical ingredients

The first selected API is **ibuprofen**, systematically 2-(4-Isobutylphenyl)propanoic acid ($C_{13}H_{18}O_2$) as an example of a widely used analgesic-antipyretic-antiflammator drug. The racemic mixture is commonly used in medical treatment, whereas the S- enantiomer has stronger pharmaceutical activity than the R- enantiomer, which is metabolically transformed to S- in the organism. [10] In this work the S- form, which is visualised in Figure 2, is used. The molar weight is $M_w = 206.28 \, \text{g} \, \text{mol}^{-1}$ and the melting point is 324.4 K. [11]

The second selected API is **naproxen**, systematically 2-(6-Methoxynaphthalen-2-yl)propanoic acid ($C_{14}H_{14}O_3$), a non-steroidal anti-inflammatory drug, used as a painkiller. Naproxen contains three oxygen atoms (one carboxyl group and one ether bond), the structure is shown in Figure 2 in the upper right corner. On the basis of its structure, naproxen can donate one hydrogen bond and accept up to three

hydrogen bonds. Naproxen is a white crystalline powder, with a molar weight of $M_w = 230.263$ g mol^{-1} and melting point 429.3 K. [11]

Carbamazepine, alternatively 5-Carbamoyl-5H-dibenzo(b,f)azepine ($C_{15}H_{12}N_2O$) is a representative anticonvulsant, which is used for the treatment of seizures and neuropathic pain. Carbamazepine contains two nitrogen atoms (amide group) and one oxygen in the carboxyl group; its structure is shown in Figure 2 on the left side. According to its structure, carbamazepine can accept and donate one hydrogen bond. Carbamazepine is a white crystalline powder, with a molar weight of $M_w = 236.273$ g mol^{-1} and melting temperature of 463.6 K. [11]

indomethacin, 2-1-[(4-Chlorophenyl)carbonyl]-5-methoxy-2-methyl-1H-indol-3-ylacetic acid ($C_{19}H_{16}ClNO_4$), which structure is in Figure 2, is used in the treatment of musculoskeletal and joint disorders. The molar weight is $M_w = 357.8$ g mol^{-1} and the melting temperature is 433.3 K. [11]
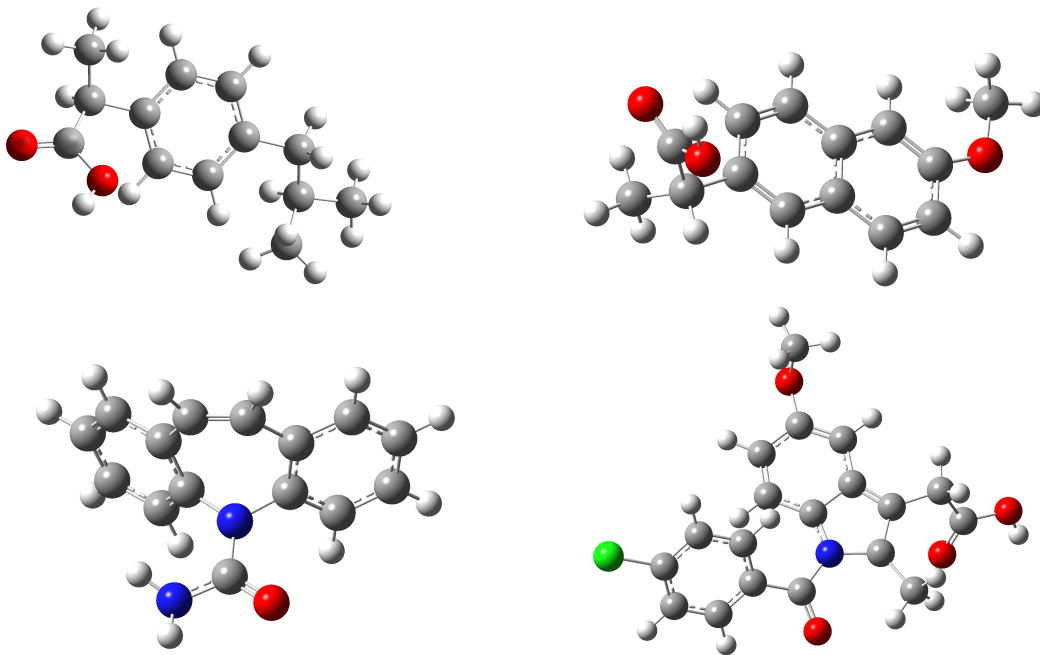

Figure 2: Molecular structures of ibuprofen (**top left**), naproxen (**top right**), carbamazepine (**bottom left**) and indomethacin (**bottom right**).

The last selected API was **sulfathiazole** with systematic name 4-amino-N-thiazol-2-ylidenebenzene-sulfonamide as a representative antibiotic drug from the sulfonamides group, which is used in the treatment of pyogenic cutaneous infections. Sulfathiazole is a white crystalline powder, with a molar weight (M_w) =255.3 gmol^{-1}, which is highly polymorphic, five polymorphs have been discovered so far [6]. All known polymorphs of sulfathiazole crystallise in the $P2_1/c$ space group, but there are differences in intermolecular bonding and structural properties [12]. The

II polymorph structure, shown in Figure 3, is used in this work. There are four molecules of sulfathiazole in the crystal monoclinic unit cell.
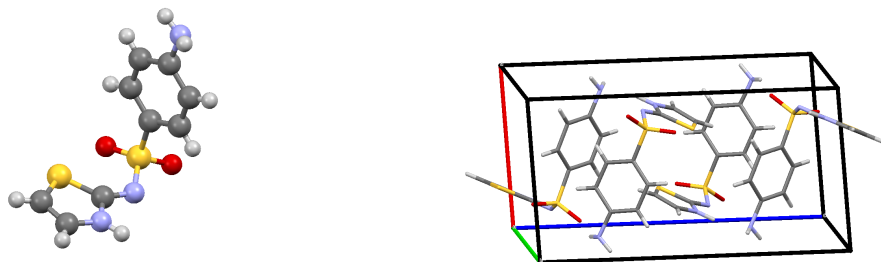

Figure 3: Sulfathiazole - molecular structure on the left and a unit cell of its II polymorph on the right.

1.2 Objective

2 THEORETICAL PART

2.1 Molecular dynamics

The molecular dynamics method is based on solving the equations of motion of classical Newtonian mechanics for atoms. Let us choose the assumption that the interaction potential U is continuous and differentiable. The force acting on the i particle can thus be written as an equation 2.1

$$f_i = -\frac{\partial U(r^N)}{\partial r_i}, \qquad i = 1, ..., N. \tag{2.1}$$

In molecular dynamics, we are focused on the time development of the model. In the other words, we are looking for the trajectory of the solution of the respective systems of differential equations. In Newtonian mechanics, acceleration is directly related to forces through the equations of motion. Formally, we can write the equation 2.2

$$\ddot{r}_i = \frac{f_i}{m_i}, \qquad i = 1, ..., N, \tag{2.2}$$

where the second time derivative of the positions appears on the left side. The equation 2.2 is a system of $3N$ ordinary differential equations for a set of N atoms. As initial conditions, we usually choose knowledge of all positions r_i and velocities $\dot{r}_i$ at the initial time $t = t_0$.

We solve equation 2.2 using the finite difference method when we track the desired solution in the form of the function $r_i(t), i = 1, .., N$, in the time interval $[t_0, t_{max}]$ at discrete points of the form $t = t_0 + kh$, where h is the integration step and k is a non-negative integer.

To find a solution, it is necessary to calculate the forces acting on individual particles at each step of the simulation. One of the methods that is applied in this area is the Verlet integration method. It is a simple and very effective method that provides sufficiently accurate results. Its great advantage is the reversibility of time and the conservation of the total energy of the system [13].

2.1.1 Verlet integration

Verlet integration method is a numerical method for integrating the equation 2.1. We express the second derivative using finite differences. From the second-order Taylor expansion $r_i(t \pm h)$ centred at t, we obtain the formula

$$\ddot{r}_i = \frac{r_i(t - h) - 2r_i(t) + r_i(t + h)}{h^2}, \tag{2.3}$$

binding values at three points in a row ($t - h$, t and $t + h$). We will use this characteristic to calculate $r_i(t + h)$. By substituting 2.3 into 2.1 we get

$$r_i(t + h) = 2r_i(t) - r_i(t - h) + h^2 \frac{f_i(t)}{m_i}. \tag{2.4}$$

In this formulation, we are able to calculate the new positions at time $t + h$ from knowledge of the forces at time t, the positions of the particles at time t and the previous time $t - h$. The time reversibility of the method is clearly visible here. The advantage is that the force is calculated only once in each step of the simulation. For the position preceding the initial position ($r_i(t_0 - h)$), we can use the expansion 2.5

$$r_i(t_0 - h) = r_i(t) - h\dot{r}_i(t_0) + h^2 \frac{f_i(t_0)}{2m_i}. \tag{2.5}$$

2.2 Silová pole

2.3 Polarizovaná silová pole

3   COMPUTATIONAL METHODS

LAMMPS software [14] (version 5 May 2020) was used for all molecular dynamics calculations. The placement of molecular chains in the simulation boxes was done by Packmol [15], the chains were randomly distributed in the space of a cubic box. The input files for the LAMMPS software were generated using the fftool [16] script written in the Python programming language.

We also used periodic boundary conditions in the directions of all axes and velocity Verlet integrator. Contributions of long-range charge interactions of distant atoms were calculated using the long-range solver using the particle-particle-particle mesh (PPPM) algorithm [17]. The bonds and angles were considered as harmonic oscillators, and for dihedral angles, OPLS (Optimised Potentials for Liquid Simulations) was used for every atom. Coulombic point charges and the Lennard-Jones potential were used, the cut-off distance for dispersion and Coulombic interactions was set to 12 Å. A SHAKE atom algorithm [18] was applied to constrain the lengths of covalent bonds that terminate in hydrogen atoms. The simulations were run under NPT conditions using the Nosé-Hoover thermostat and barostat [19], with relaxation times for temperature control as 100 fs and pressure control as 1000 fs. The simulations contained around 25 000 atoms in a simulation box. From previous research, this was considered to be a suitable setting. [9]

All-atom non-polarisable force fields were used during MD simulations, the parameterisation of the PLA force field was obtained from the literature [20], the parameterizations of APIs were also taken from the literature. [21]

We started all simulations with an equilibration simulation run from randomly packed simulation boxes under the temperature of 500 K and pressure of 1 bar in three blocks with a gradually increasing time-integration step. The simulation began with a step of 0.25 fs, followed by steps 0.5 and 0.75 each for a simulation time of 0.5 ns, then 1 ns of simulation with a step of 1 fs. From this point, we cooled the system, down to 300 K for 2 ns with a step of 1 fs. After this cooling, we continued with a 10 ns long production run with a temperature of 300 K and pressure equal to 1 bar.

From these production runs, we evaluated the MSD (Mean Squared Displacement) of API and PLA molecules in the mixture and the RDF (radial distribution function) of atom interactions. We also performed a production run under the higher temperature of 500 K and the same pressure of 1 bar starting from conformations after the first equilibration under 500 K. We also sampled RDFs and MSDs. Those simulations were performed for neat APIs, PLA polymer, and mixtures with differ-

ent concentrations of API. For each API, the concentration ratio API:PLA in the number of molecules was 100:17 ($x_{API} = 0.85$), 200:17 ($x_{API} = 0.92$), and 300:17 ($x_{API} = 0.95$).

To determine the glass transition temperature (T_g) of the mixtures, we performed simulated annealing simulations with a gradually decreasing temperature (30 K· ns^{-1}) starting at 800 K and ending at 200 K. Systems containing a mixture of API and PLA were first warmed from 500 K to 800 K for 2 ns. To have statistically more reliable data, simulated annealing simulations were performed from 5 different initial conformations. The 4 ns long run was done to obtain those conformations sampling the image of the box every 1 ns.

4 RESULTS AND DISCUSSION

4.1 Simulations of API

The box of neat carbamazepine contained 800 molecules (24 000 atoms), after equilibration run, the size of the box was 66 Å. In the naproxen simulation box 800 molecules were presented (24 800 atoms), balanced box size was 66 Å.

4.2 Simulations of polymers

4.3 Sulfathiazol ruzna pole

4.4 Simulace smesi

4.4.1 dodatkove energie a objemy

4.4.2 RDF

4.4.3 porovnani API a API se se smesi, vznamne kontakty

4.4.4 MSD

4.4.5 Tg skelny prechod

4.5 Smesi s polarizovanym polem

5 CONCLUSION

text

References

1. Leuner, C. Improving drug solubility for oral delivery using solid dispersions. *European Journal of Pharmaceutics and Biopharmaceutics* **2000**, *50*, 47–60.

2. Batisai, E. Solubility Enhancement of Antidiabetic Drugs Using a Co-Crystallization Approach. *ChemistryOpen* **2021**, *10*, 1260–1268.

3. Huang, L. Impact of solid state properties on developability assessment of drug candidates. *Advanced Drug Delivery Reviews* **2004**, *56*, 321–334.

4. Srinarong, P.; De Waard, H.; Frijlink, H. W.; Hinrichs, W. L. Improved dissolution behavior of lipophilic drugs by solid dispersions: the production process as starting point for formulation considerations. *Expert Opinion on Drug Delivery* **2011**, *8*, 1121–1140.

5. Vasconcelos, T.; Sarmento, B.; Costa, P. Solid dispersions as strategy to improve oral bioavailability of poor water soluble drugs. *Drug Discovery Today* **2007**, *12*, 1068–1075.

6. Caron, V.; Tajber, L.; Corrigan, O. I.; Healy, A. M. A Comparison of Spray Drying and Milling in the Production of Amorphous Dispersions of Sulfathiazole/Polyvinylpyrrolidone and Sulfadimidine/Polyvinylpyrrolidone. *Molecular Pharmaceutics* **2011**, *8*, 532–542.

7. Prudic, A.; Ji, Y.; Sadowski, G. Thermodynamic Phase Behavior of API/Polymer Solid Dispersions. *Molecular Pharmaceutics* **2014**, *11*, 2294–2304.

8. Newman, A.; Zografi, G. What Are the Important Factors That Influence API Crystallization in Miscible Amorphous API-Excipient Mixtures during Long-Term Storage in the Glassy State? *Molecular pharmaceutics* **2022**, *19*, 378–391, Place: United States.

9. Klajmon, M.; Aulich, V.; Ludík, J.; Červinka, C. Glass Transition and Structure of Organic Polymers from All-Atom Molecular Simulations. *Industrial & Engineering Chemistry Research* **2023**, *62*, 21437–21448.

10. Rainsford, K. D. Ibuprofen: pharmacology, efficacy and safety. *Inflammopharmacology* **2009**, *17*, 275–342.

11. Štejfa, V.; Pokorný, V.; Mathers, A.; Růžička, K.; Fulem, M. Heat capacities of selected active pharmaceutical ingredients. *The Journal of Chemical Thermodynamics* **2021**, *163*, 106585.

12. Drebushchak, T. N.; Boldyreva, E. V.; Mikhailenko, M. A. Crystal structures of sulfathiazole polymorphs in the temperature range 100–295 K: A comparative analysis. *Journal of Structural Chemistry* **2008**, *49*, 84–94.

13. Nezbeda, I.; Kolafa, J.; Kotrla, M. *Úvod do počítačových simulací:metody Monte*

Carlo a molekulární dynamiky.; Karolinum, 1998.

14. Thompson, A. P.; Aktulga, H. M.; Berger, R.; Bolintineanu, D. S.; Brown, W. M.; Crozier, P. S.; In 'T Veld, P. J.; Kohlmeyer, A.; Moore, S. G.; Nguyen, T. D.; Shan, R.; Stevens, M. J.; Tranchida, J.; Trott, C.; Plimpton, S. J. LAMMPS - a flexible simulation tool for particle-based materials modeling at the atomic, meso, and continuum scales. *Computer Physics Communications* **2022**, *271*, 108171.

15. Martínez, L.; Andrade, R.; Birgin, E. G.; Martínez, J. M. P ACKMOL : A package for building initial configurations for molecular dynamics simulations. *Journal of Computational Chemistry* **2009**, *30*, 2157–2164.

16. Padua, A. ENS Lyon, France. `https://github.com/paduagroup/fftool`.

17. Hockney, R.; Eastwood, J. *Computer Simulation Using Particles*, 0th ed.; CRC Press, 2021; p 540.

18. Ryckaert, J.-P.; Ciccotti, G.; Berendsen, H. J. Numerical integration of the cartesian equations of motion of a system with constraints: molecular dynamics of n-alkanes. *Journal of Computational Physics* **1977**, *23*, 327–341.

19. Tuckerman, M. E.; Alejandre, J.; López-Rendón, R.; Jochim, A. L.; Martyna, G. J. A Liouville-operator derived measure-preserving integrator for molecular dynamics simulations in the isothermal–isobaric ensemble. *Journal of Physics A: Mathematical and General* **2006**, *39*, 5629–5651.

20. McAliley, J. H.; Bruce, D. A. Development of Force Field Parameters for Molecular Simulation of Polylactide. *Journal of Chemical Theory and Computation* **2011**, *7*, 3756–3767.

21. Červinka, C.; Fulem, M. Structure and Glass Transition Temperature of Amorphous Dispersions of Model Pharmaceuticals with Nucleobases from Molecular Dynamics. *Pharmaceutics* **2021**, *13*, 1253.

List of Abbreviations

x position

v velocity

...

List of Symbols

x position

v velocity

...

List of Tables

List of Figures

Appendix A   Headline